Effects of long-range interactions on curvature energies of viral shells

Hamid R. Shojaei,[1,*] Anže Lošdorfer Božič,[2,†] Murugappan Muthukumar,[3,‡] and Rudolf Podgornik[1,2,4,§]

[1]*Department of Physics, University of Massachusetts, Amherst, Massachusetts 01003, USA*

[2]*Department of Theoretical Physics, J. Stefan Institute, Ljubljana, Slovenia*

[3]*Department of Polymer Science and Engineering, Materials Research Science and Engineering Center, University of Massachusetts, Amherst, Massachusetts 01003, USA*

[4]*Department of Physics, Faculty of Mathematics and Physics, University of Ljubljana, Ljubljana, Slovenia*

(Received 9 February 2016; revised manuscript received 2 May 2016; published 23 May 2016)

We formulate a theory of the effects of long-range interactions on the surface tension and spontaneous curvature of proteinaceous shells based on the general Deryaguin-Landau-Verwey-Overbeek mesoscale approach to colloid stability. We derive the full renormalization formulas for the elastic properties of the shell and consider in detail the renormalization of the spontaneous curvature as a function of the corresponding Hamaker coefficient, inner and outer capsid charges, and bathing solution properties. The renormalized spontaneous curvature is found to be a nonmonotonic function of several parameters describing the system.

DOI: 10.1103/PhysRevE.93.052415

I. INTRODUCTION

It has recently become clear that long-range interactions are extremely important also in the self-assembly of capsid proteins into viral shells and that they determine the self-assembly phase diagram [1]. Electrostatic interactions that originate in the effective charge on the capsid proteins [2], as governed by the pH and the ionic strength of the bathing solution, can fundamentally change the phase diagram of the capsid protein of the cowpea chlorotic mottle virus (CCMV), yielding single-wall and multiwall capsids, as well as tubes and free protein [3]. These results seem to implicate that a change in the spontaneous curvature of the capsid as a function of the charge asymmetry of the proteinaceous shell as well as the solution conditions regulates the size of the shell [4,5]. We thus focus our attention on precisely how, in the context of empty capsid shells, the long-range electrostatic and van der Waals (vdW) interactions *together* conspire to modulate the mesoscopic properties of spheroidal aggregates, specifically their spontaneous curvature.

Standard principles of colloid and nanoscale stability theory in fact identify *grosso modo* two types of interactions that together govern the self-assembly and disassembly of biological macromolecules and their molecular aggregates [6]: the electrostatic interactions depending on the specific nature of molecular charges [7] and the ubiquitous vdW interactions depending on the dielectric response properties of molecular material [8,9]. This is also the most fundamental assertion of the DLVO (Deryaguin-Landau-Verwey-Overbeek) theory of macromolecular stability [10]. When macromolecular aggregates are net charged, the ensuing (screened) Coulomb interactions between identical molecules are usually repulsive, with solvent effects due to hydrophillic moieties contributing an additional short-range component to the overall molecular repulsions [11]. On the other hand, neutral molecular aggregates usually interact via nonspecific vdW attractions [12], augmented again by the solvent effects engendered by the hydrophobic moieties along the solvent-exposed surfaces [13]. In fact, in the context of proteins, the interactions are mostly entropy driven [14,15], usually interpreted to originate in water-mediated hydrophobic interactions. As part of the vdW interactions, the s.c. zero frequency term is also entropic in origin; it is with some difficulty that one can differentiate between this part of the vdW interactions and the hydrophobic interactions proper [16]. Of these four interactions hydrophobic and/or hydration forces correspond to an effective interaction arising from the statistical properties of water molecules around the dissolved macromolecular moieties, while the electrostatic and vdW forces are indeed "true" forces that act even in the absence of any solvent. The overall stability condition then proceeds from comparing the strengths of these interactions.

Since the bathing solution in the biological milieu contains various dissolved ionic species the electrostatic interaction depends on its exact composition [17], i.e., the concentration and valency of salt ions due to Debye-Hückel screening, but also on the amount of charge they carry, which can be modified by shifting the dissociation equilibrium via the solution pH [18,19]. At the same time the vdW interaction is a complicated functional of the dielectric response function of the components of the macromolecular aggregates [8] as well as of the bathing solvent, which can be modified by solutes, e.g., low molecular weight solutes such as glucose and sucrose [20].

While there are obvious similarities, there are nevertheless fundamental differences between the elasticity of rigid proteinaceous shells of tethered capsomeres [21] and that of spheroidal lipid vesicles which are composed of a quasi-two-dimensional fluid layer of lipid molecules [22]. The electrolytes on the two sides of an impermeable membrane can, in principle, differ, an assumption usually unrealistic for viral shells, which are typically completely permeable to various ionic species (however, see Ref. [23]). The contribution of electrostatic interactions to spontaneous curvature as well as the bending rigidity renormalization of lipid membranes was analyzed in standard fashion within the mean-field

*hshojaei@physics.umass.edu
†anze.bozic@ijs.si
‡muthu@polysci.umass.edu
§podgornik@physics.umas.edu

Poisson-Boltzmann (PB) framework, starting from the seminal work of Winterhalter and Helfrich [24] and later generalized to more realistic scenarios [25–30]. In what follows we also delimit ourselves to monovalent electrolytes described at the level of the mean-field PB theory. Though the effects of multivalent electrolytes have been studied in standard fashion on the PB level [29], they cannot in general be analyzed within the mean-field framework [17] and lead to instabilities which have no counterpart in the behavior of the monovalent salts [31]. The contribution of vdW interactions to spontaneous curvature and bending rigidity renormalization of lipid membranes has also been extensively analyzed on a variety of levels, starting with the approach of Parsegian and Weiss, based on Lifshitz theory of vdW interactions [32], and later generalized at different levels [33–38].

The main differences between the two-dimensional fluid layer of soft lipid molecules and crystal-like assemblies of tethered capsomers boil down to the fact that the latter are usually permeable to salt ions (even to larger ones), being in thermodynamic equilibrium with the bulk reservoir, which sets the ions' chemical potential. The effective surface charge density of capsomers can thus be viewed as highly constrained and as not responding to small curvature deformations. These specific features of proteinaceous shells lead to important differences and make the available theoretical results valid for lipid layers, in general, not applicable. We consider spherical shells only and calculate the contribution of vdW interactions to spontaneous curvature on the level of the Lifshitz theory for general asymmetric layers and, at the same time, use the linearized PB theory to evaluate also the contribution of asymmetric charged shells with a fixed surface charge density. This will allow us to derive the full DLVO expression for the change in the spontaneous curvature while assuming a known experimentally determined value for the bending rigidity. In this way, we bypass the unknown position of the "neutral surface," which actually changes the exact renormalization of the bending rigidity only (see below).

II. THEORY

A. Curvature expansion of the free energy

We analyze a thin spheroidal charged shell and expand its vdW-Lifshitz interaction free energy as well as its electrostatic free energy in terms of the reciprocal radius of curvature R. The total interaction free energy of the spheroidal shell can be written as

$$\mathcal{F} = \int_S \mathrm{d}S\left(\sigma_0 + \frac{a}{R} + \frac{b}{R^2} + \dots\right), \tag{1}$$

where S is the area of the shell, dS is its element, and σ_0, a, and b are constants that depend on the details of the long-range interactions. This expansion should be compared with the mesoscopic elastic deformation free energy [39],

$$\mathcal{F} = \int_S \mathrm{d}S\left(\sigma + \frac{1}{2}K_c\left(\frac{1}{R} - \frac{1}{R_0}\right)^2 + \dots\right), \tag{2}$$

where σ is the surface tension, K_c is the bending rigidity, and R_0 is the spontaneous radius of curvature, allowing us to identify the interaction renormalization of the mesoscopic bending rigidity and spontaneous radius of curvature as

$$\sigma \longrightarrow \sigma_0 + \frac{K_c}{R_0^2}, \quad K_c \longrightarrow K_c + 2b, \quad \frac{1}{R_0} \longrightarrow \frac{1}{R_0} - \frac{a}{K_c}. \tag{3}$$

All the mesoscopic parameters of shell elasticity thus contain a bare part, due to short-range interactions, that is not taken into account specifically, and a renormalized long-range DLVO interactions part, just as in the case of semiflexible polyelectrolytes [40]. While the electrostatic renormalization of mesoscopic elasticity parameters has been analyzed at various levels of sophistication (see above), the complete DLVO assessment of elastic parameter renormalization has not been properly addressed.

It is obvious from the expansion, Eq. (1), that, depending on how we define the origin of the radius of curvature, or by making the substitution $R \longrightarrow R + \delta R$, part of the a coefficient can migrate into the b coefficient and thus the renormalization of the bending rigidity depends on the details of the deformation process, i.e., what part of the layer remains unaffected by the deformation and the exact position of this "neutral surface." In order to avoid this ambiguity in the definition of the bending rigidity renormalization, we concentrate purely on the spontaneous curvature and the surface tension, taking the bending rigidity as an empirical parameter. A similar indeterminacy has been noted also in the context of membrane electrostatics [29], where the results on the bending rigidity renormalization depend on the details of the deformation process. We derive the first two terms of the curvature expansions of both the vdW interactions on the level of the macroscopic Lifshitz theory and the electrostatic interactions on the level of the Deby-Hückel theory. As will become obvious, both of them can be derived in an explicit analytic form suitable for relevant numerical computations.

B. Curvature expansion of the vdW-Lifshitz interaction

The Lifshitz theory of vdW interactions connects the dielectric response function at imaginary frequencies, $\epsilon(i\zeta)$, defined via the imaginary part of the dielectric response function $\epsilon''(\omega)$, as [41]

$$\varepsilon(i\zeta) = 1 + \frac{2}{\pi}\int_0^\infty \frac{\omega\varepsilon''(\omega)}{\omega^2 + \zeta^2}d\omega, \tag{4}$$

with the interaction free energy between the materials described by this dielectric response [8]. The connection is via the fluctuation-dissipation theorem and the Lifshitz theory actually evaluates the free energy contribution of all the electromagnetic-field fluctuations. We consider the vdW interactions across a curved parallel single-layer system that will mimick a thin spherical curved molecular sheet. In the derivation of the curvature expansion we modify the original methods of Weiss, Parsegian, and Witte [32,35] based on the Lifshitz theory.

The vdW free energy of this system depends on the dielectric mismatch $\Delta(i\zeta)$ at the inner and outer boundaries of the thin spherical sheet of inner radius R and thickness

$w \ll R$, i.e.,

$$\Delta_{32}(i\zeta) = \frac{\epsilon_3(i\zeta) - \epsilon_2(i\zeta)}{\epsilon_3(i\zeta) + \epsilon_2(i\zeta)}, \qquad \Delta_{21}(i\zeta) = \frac{\epsilon_2(i\zeta) - \epsilon_1(i\zeta)}{\epsilon_2(i\zeta) + \epsilon_1(i\zeta)}. \tag{5}$$

Here, by assumption, the dielectric response of the shell is that of the capsid proteins, $\epsilon_2(i\zeta) = \epsilon_p(i\zeta)$, and $\epsilon_3(i\zeta) = \epsilon_1(i\zeta) = \epsilon_w(i\zeta)$ is the dielectric response of the aqueous solvent. Dielectric response functions at imaginary frequencies $\epsilon_k(i\zeta)$ are obtained from a Kramers-Kronig transform of the imaginary part of the dielectric function in a standard way [8], once one either chooses a model for the frequency response or measures it directly for a particular material. While the frequency response of capsid proteins is presently not (yet) available, it exists for many other materials [12]. It is obvious that for any value of the argument as well as any model one should have $-1 < \Delta_{ij}(i\zeta) < 1$.

In the Lifshitz theory of vdW interactions the free energy for a single-spherical-parallel-layer system can be calculated in a closed form as a sum over the log of the secular determinant, $\mathcal{D}(\omega, \mathbf{k}; g)$, whose zeros on the real-frequency ω axis yield the wave vector $\mathbf{k}$–dependent frequencies of the eigenmodes of Maxwell's equation in the chosen interaction geometry as a function of the parameters describing that geometry g [8]. The vdW-interaction free energy can then be derived in the general form

$$\mathcal{G}_{\rm vdW} \equiv \sum_{N=0}^{\infty}{}' \sum_{\mathbf{k}} \log\left(\mathcal{D}(i\zeta_N, \mathbf{k}; g)\right), \tag{6}$$

where the sums are over the geometry-dependent set of wave vectors $\mathbf{k}$ and over the thermal Matsubara frequencies $\zeta_N = 2\pi N k_B T/\hbar$, where N is an integer, and $k_B T$ and $\hbar$ are the thermal energy and Planck's constant, respectively. The $N = 0$ term is counted with a weight of $1/2$, indicated by the prime on the sum. The Matsubara sum, embodying the finite-temperature effects, is trivial and can be done numerically for a chosen model of the frequency dependence of the dielectric response function.

For a single-sphericalparallel-layer system, of thickness w and inner shell radius R, this general formula is reduced to [32,35]

$$\mathcal{G}_{\rm vdW}(R, w, \Delta_{32}, \Delta_{21}) = \sum_{N=0}^{\infty}{}' \mathcal{G}_N(R, w, \Delta_{32}(i\zeta_N), \Delta_{21}(i\zeta_N)), \tag{7}$$

where we have defined the single Matsubara frequency free energy function

$$G_N(R, w, \Delta_{32}(i\zeta), \Delta_{21}(i\zeta)) = k_B T \sum_{\ell=0}^{\infty} (2\ell+1) \ln\left[1 + \frac{4\ell(\ell+1)\Delta_{32}\Delta_{21}\left(1+\frac{w}{R}\right)^{-(2\ell+1)}}{(2\ell+1+\Delta_{32})(2\ell+1+\Delta_{21})}\right] = \sum_{\ell=0}^{\infty} G^{(\ell)}(R, w; N), \tag{8}$$

which can be obtained from the solutions of the Maxwell equations in the spherical shell geometry [32,35]. The only remaining "wave vector" in the sum, Eq. (6), is then the degree ℓ of the spherical harmonic function.

Since what we want is an expansion in curvature up to the second order, Eq. (1), we only consider terms in the above free energy up to that order. In what follows we analyze the R and w dependence of $G_N(R, w, \Delta_{32}(i\zeta), \Delta_{21}(i\zeta))$ by modifying the previous method [35]. Using the Euler-Maclaurin summation formula, we transform Eq. (9) into

$$\sum_{\ell=0}^{\infty} G^{(\ell)}(R, w; N) = \int_0^{\infty} d\ell\, G^{(\ell)}(R, w; N) - \frac{1}{12} G'^{(0)}(R, w; N) + \ldots, \tag{9}$$

where the other terms either are 0 or do not contribute to the order R^{-2}. We next introduce the variable $l = xR/w$ and keep terms to the second order, i.e., to $(w/R)^2$, as assumed in our curvature expansion, Eq. (1). This yields the expansion for the surface free energy density

$$\frac{1}{4\pi R^2}\mathcal{G}_{\rm vdW}(R, w, \Delta_{32}, \Delta_{21}) = k_B T \sum_{N=0}^{\infty}{}' \left[F_0(\Delta^*, \overline{\Delta}; w) + \frac{1}{R} F_1(\Delta^*, \overline{\Delta}; w) + \frac{1}{R^2}(F_2(\Delta^*, \overline{\Delta}) + \tilde{F}_2(\Delta^*, \overline{\Delta}; w))\right], \tag{10}$$

with the definitions

$$F_0(\Delta^*, \overline{\Delta}; w) = \frac{1}{2\pi w^2} \int_0^{\infty} dx\, x \ln(1 + \Delta^* e^{-2x}) = -\frac{1}{8\pi w^2} \mathrm{Li}_3(\Delta^*), \tag{11}$$

$$F_1(\Delta^*, \overline{\Delta}; w) = = \frac{1}{4\pi w}\left[\int_0^{\infty} dx \ln(1 + \Delta^* e^{-2x}) + \int_0^{\infty} dx \frac{\Delta^* e^{-2x}}{1 + \Delta^* e^{-2x}}(x^2 - x - \overline{\Delta})\right] = \frac{1}{4\pi w} \tilde{f}_1(\Delta^*, \overline{\Delta}), \tag{12}$$

$$F_2(\Delta^*, \overline{\Delta}) = \frac{1}{24\pi} \int_0^{\infty} dx \frac{\Delta^* e^{-2x}}{(1 + \Delta^* e^{-2x})^2}((6x^3 - 20x^2 + 6x(3 - \overline{\Delta}) - 6(1 - \overline{\Delta})) - \Delta^* e^{-2x}(8x^2 - 12x + 6)) - \frac{\Delta^*}{12\pi(1 + \overline{\Delta} + \Delta^*)} \tag{13}$$

and

$$\tilde{F}_2(\Delta^*,\overline{\Delta};w) = -\frac{1}{48\pi}\int_0^\infty \frac{dx}{x}\frac{\Delta^* e^{-2x}}{(1+\Delta^* e^{-2x})^2}(6(1+\Delta^*-\overline{\Delta}^2)+\Delta^* e^{-2x}(6+6\Delta^*-3\overline{\Delta}^2))$$
$$\simeq \frac{\Delta^*(6(1+\Delta^*-\overline{\Delta}^2)+\Delta^*(6+6\Delta^*-3\overline{\Delta}^2))}{48\pi(1+\Delta^*)^2}\log\frac{w}{a}, \tag{14}$$

where

$$\overline{\Delta} = \Delta_{32}+\Delta_{21} = \Delta_{wp}+\Delta_{pw},$$
$$\Delta^* = \Delta_{32}\,\Delta_{21} = \Delta_{wp}\,\Delta_{pw}. \tag{15}$$

This is now the final expression for the vdW free energy expansion in terms of the inverse radius. All the integrals in the above expression can in fact be calculated explicitly and analytically via the Lerch function (see the Appendix). The implied Matsubara summation can, finally, be taken for any concrete model of the dielectric response. The lowest order term, containing the integral of $F_0(\Delta^*,\overline{\Delta};w)$, is identical to the vdW free energy of interaction between semi-infinite media 1 and 3 across the plane-parallel slab of medium 2, scaling as the inverse second power of the thickness of the slab, w [8].

The logarithmic divergence of $\tilde{F}_2(\Delta^*,\overline{\Delta};w)$ is consistent with the previous results on the renormalization of the bending rigidity to the lowest order in the dielectric mismatch [33], while formula (14) presents the full Lifshitz result to all orders in the dielectric mismatch. Of the three terms in Eq. (10), we concentrate only on the first two. The first pertains to the renormalization of the surface free energy where its bare value, stemming from short-range interactions between the capsid proteins, is unknown, while the third term, describing the bending rigidity renormalization, allows for an ambiguity because—depending on the definition of the "neutral surface"—it contains an undefined constant. We thus take the full, renormalized value of the bending rigidity as an empirical constant.

C. Curvature expansion of the electrostatic interaction

The PB theory of electrostatic interactions sets the framework for calculation of the curvature expansion of the electrostatic part of the free energy [7]. In the model considered, based on the rigid nature of the proteinaceous virus shell, we assume a fixed surface charge density at the inner and at the outer boundary of the shell, which can, nevertheless, differ [2]. We also assume a different static dielectric permittivity for the shell than for the bathing aqueous solution in which the shell is immersed, following closely the approach in Ref. [42]. Again, we delimit ourselves to the surface tension and the spontaneous curvature term, for the same reasons as already invoked in the context of the vdW interaction.

The inner radius of a charged shell is again taken as R, with surface charge density σ_1, and the outer radius as $R+w$, with surface charge density σ_2. Both can be extracted from a detailed statistical analysis of the VIPERdb for different virus families [43]. The majority of analyzed viruses tend to have a slightly negative σ_2. The charge on the inner shell is, however, less universal and most of the analyzed viruses have either a negative or a positive σ_1. This conclusion has to be amended if one adds disordered N-tails of the proteins on the inner surface that shift the inner shell charge to more positive values (for details see Ref. [43]), strongly influencing also the stable length of the encapsidated genome [44].

We are seeking again an expansion of the free energy up to the second order in terms of the inverse powers of the inner radius of curvature R, again assuming that $w \ll R$. The static dielectric constant of water is ε_w, and those of the of the capsid protein $\varepsilon_p < \varepsilon_w$ are taken as $\varepsilon_p = 5$ and $\varepsilon_w = 80$. Additionally, we denote $\mu = \varepsilon_p/\varepsilon_w < 1$.

In what follows we delimit ourselves exclusively to the linearized PB (Debye-Hückel; DH) theory within its range of validity [7]. The electrostatic part of the free energy is then given as a functional of the mean-field electrostatic potential, $\varphi(\mathbf{r})$, in the form

$$\mathcal{G}_{el} = \frac{1}{2}\varepsilon_w\varepsilon_0\int_{(V)}((\nabla\varphi(\mathbf{r}))^2+\kappa^2\varphi(\mathbf{r})^2)d^3\mathbf{r}$$
$$= \varepsilon_w\varepsilon_0\oint_{(S=\partial V)}\varphi(\mathbf{r}_S)(\mathbf{n}\cdot\nabla\varphi(\mathbf{r}_S))d^2\mathbf{r}_S. \tag{16}$$

κ is the inverse Debye screening length set by the ionic strength of the monovalent salt of concentration c_0 in the regions $r < R$ and $r > R+w$, i.e., $\kappa^2 = 2\beta e^2 c_0/(\varepsilon_0\varepsilon_w)$, and is the same inside and outside the shell, whereas within the shell $\kappa \equiv 0$. For a spherical shell of thickness w and inner radius R, the mean-field electrostatic potential by assumption depends only on the radial coordinate, $\varphi(\mathbf{r}) = \varphi(r)$, and satisfies either the DH equation or the Laplace equation,

$$\nabla^2\varphi(r) = \kappa^2\varphi(r) \quad \text{or} \quad \nabla^2\varphi(r) = 0 \quad \text{for} \quad R \leqslant r \leqslant R+w. \tag{17}$$

These two equations have to be solved with appropriate boundary conditions, i.e., $\varepsilon_w\varepsilon_0\partial_r\varphi$ $(r = R)$ has a jump equal to σ_1, and $\varepsilon_w\varepsilon_0\partial_r\varphi$ $(r = R+w)$ a jump equal to σ_2. The overall form of the mean-field electrostatic potential on r is very similar to the one displayed in Fig. 5 of Ref. [42].

While one could formally extend the PB theory to multivalent salts [29], the results could not be properly validated at the mean-field level [17] and led to additional considerations that are not addressed here [31]. Furthermore, we work exclusively in the grand canonical ensemble, where the screening parameters of the electrolyte are set by the bulk reservoir, a straightforward consequence of the fact that the viral capsids are usually completely permeable to salt, as opposed to lipid vesicles, where the number of salt ions in the interior can be constrained [29].

Within the limit of the DH theory for spherically symmetric shells, the electrostatic free energy, Eq. (16), for a charged shell

of thickness w, as defined above, can be rewritten as [27]

$$\mathcal{G}_{\rm el} = \varepsilon_w \varepsilon_0 \oint_{(S=\partial V)} \varphi(\mathbf{r}_S)(\mathbf{n}\cdot\nabla\varphi(\mathbf{r}_S))d^2\mathbf{r}_S = \frac{1}{2}4\pi R^2\,\sigma_1\,\varphi(R) + \frac{1}{2}4\pi(R+w)^2\,\sigma_2\,\varphi(R+w), \quad (18)$$

where the mean-field electrostatic potential can be obtained from the solutions of the DH equation outside the proteinaceous layer and from the Laplace equation inside, Eq. (17), since the proteinaceous shell itself is impenetrable to ions, with the boundary conditions specified above. The general solution of this problem can be obtained analytically but we will only use the expansion in terms of R to the second order.

The final form of the free energy, Eq. (18), for this particular geometry can then be derived as

$$\mathcal{G}_{\rm el} = \frac{2\pi R^2}{\kappa\varepsilon_0\varepsilon_w}\left(\sigma_1\frac{M}{L} + \sigma_2\frac{N}{L}\right), \quad (19)$$

where the general forms of M, N, and L are derived in Ref. [42] and are related to the electrostatic potential at the two boundaries.

To second order in $1/\rho = 1/(\kappa R)$ we can simplify the general expressions for the electrostatic potential and, after some algebra, obtain the following form of the three terms in the inverse curvature expansion:

$$L = (2\mu + (\kappa w)) \times \left(1 + \frac{(\kappa w)}{\rho} + \frac{(\kappa w)^2}{\rho^2}\left[\frac{((\kappa w)+1)(\mu-1)}{(\kappa w)(2\mu+(\kappa w))}\right]\right), \quad (20)$$

$$M = (\mu(\sigma_1+\sigma_2) + (\kappa w)\sigma_1) + \frac{(\kappa w)}{\rho}(((\kappa w)+1)\sigma_1 + 2\mu\sigma_2) + \frac{(\kappa w)^2}{\rho^2}\mu\sigma_2, \quad (21)$$

and

$$N = (\mu(\sigma_1+\sigma_2) + (\kappa w)\sigma_2) + \frac{(\kappa w)}{\rho}(2\mu\sigma_1 + (4\mu + 3(\kappa w) - 1)\sigma_2) + \frac{(\kappa w)^2}{\rho^2}(\mu\sigma_1 + 3(2\mu + (\kappa w) - 1)\sigma_2). \quad (22)$$

In fact the only place where the curvature expansion needs to be taken into account is in the last expression, N, everything else being exact. This allows us to derive the final expression for the curvature expansion of the electrostatic part of the surface free energy density as

$$\frac{1}{4\pi R^2}\mathcal{G}_{el}(\sigma_1,\sigma_2,\kappa,w) = \frac{1}{2\kappa\varepsilon_0\varepsilon_w}\left(f_0(\sigma_1,\sigma_2,\kappa,w) + \frac{f_1(\sigma_1,\sigma_2,\kappa,w)}{\kappa R} + \frac{f_2(\sigma_1,\sigma_2,\kappa,w)}{(\kappa R)^2}\right), \quad (23)$$

where we have introduced the shorthand

$$f_0(\sigma_1,\sigma_2,\kappa,w) = \frac{\mu(\sigma_1+\sigma_2)^2 + (\kappa w)\left(\sigma_1^2+\sigma_2^2\right)}{2\mu + (\kappa w)}, \quad (24)$$

$$f_1(\sigma_1,\sigma_2,\kappa,w) = (\kappa w)\left(\frac{(3\mu + 2(\kappa w) - 1)\sigma_2^2 + 2\mu\sigma_1\sigma_2 - (\mu-1)\sigma_1^2}{2\mu + (\kappa w)}\right), \quad (25)$$

and

$$f_2(\sigma_1,\sigma_2,\kappa,w) = \frac{\kappa w}{(2\mu+(\kappa w))^2}\big((\mu-1)[(\kappa w)(\mu-1) - \mu]\sigma_1^2 - 2\mu((\kappa w)+1)(\mu-1)\sigma_1\sigma_2 + [(\kappa w)^3 + (\kappa w)^2(4\mu-1) + (\kappa w)(5\mu^2 - 4\mu + 1) - \mu(\mu-1)]\sigma_2^2\big). \quad (26)$$

In general, the above free energy density is not symmetric at the two surface charge densities, which were assumed to be constant during the deformation. As already stated this seems a reasonable assumption in the context of the rigid proteinaceous shells but cannot be invoked in the context of symmetric lipid vesicles [29]. In the latter case the lipid membrane is, to a good approximation, impermeable to water as well as to hydrated ions and thus represents an impermeable barrier that decouples the two compartments, a situation very much opposite to the case of a porous proteinaceous capsid.

In the limit of vanishing thickness $w \to 0$ we then obtain straightforwardly $\lim_{w\to 0}\mathcal{G}_{\rm el}(\sigma_1,\sigma_2,\kappa,w) = \pi(\sigma_1+\sigma_2)^2R^2/\kappa\varepsilon_w\varepsilon_0$, which is the correct expression for a single shell of radius R and surface charge $\sigma_0 = \sigma_1 + \sigma_2$. This corresponds to the dielectrically transparent case of Duplantier [28], considered before. Perhaps more interesting is the fact that the higher order terms are asymmetric in terms of σ_1 and σ_2. Our analysis takes fully into account the coupling between the inner and the outer layer of the proteinaceous shell and we made no approximation to decouple the two [45].

D. Combining the electrostatic and vdW interactions

We can now write the curvature expansion for the total free energy. Adding Eq. (10) and Eq. (23) will give us the terms in the free energy expansion: R^0, R^{-1}, and R^{-2}. This total surface free energy density then leads to the following interaction renormalization of the surface tension, spontaneous

radius of curvature, and mesoscopic bending rigidity:

$$\sigma \longrightarrow \sigma_0 + \frac{K_c}{R_0^2} + k_B T \sum_{N=0}^{\infty}{}' F_0(\Delta^*, \overline{\Delta}; w) + \frac{1}{2\kappa\varepsilon_0\varepsilon_w} f_0(\sigma_1, \sigma_2, \kappa, w), \tag{27}$$

$$\frac{1}{R_0} \longrightarrow \frac{1}{R_0} + \frac{1}{2K_c}\left(k_B T \sum_{N=0}^{\infty}{}' F_1(\Delta^*, \overline{\Delta}; w) + \frac{1}{2\kappa^2\varepsilon_0\varepsilon_w} f_1(\sigma_1, \sigma_2, \kappa, w)\right), \tag{28}$$

$$K_c \longrightarrow K_c + \frac{1}{2K_c}\left(k_B T \sum_{N=0}^{\infty}{}' F_2(\Delta^*, \overline{\Delta}; w) + \frac{1}{2\kappa^3\varepsilon_0\varepsilon_w} f_2(\sigma_1, \sigma_2, \kappa, w)\right). \tag{29}$$

Though we wrote down the full result for the surface energy, spontaneous curvature, and bending rigidity renormalization, we specifically investigate only the contribution of vdW and electrostatic interactions to the surface tension and spontaneous curvature of the spheroidal shell [Eq. (28)], treating the bending rigidity as a phenomenological parameter derived from experiment. As already stated, the exact form of the interaction renormalized bending rigidity depends crucially on the assumed position of the neutral surface, depending on the nature of the model one assumes for the shell. To avoid this ambiguity, we consider the value of the bending rigidity an input phenomenological parameter.

III. NUMERICAL RESULTS

The spontaneous curvature interaction renormalization depends on several parameters and we investigate specifically the dependence on the capsid charge σ_1 and the charge asymmetry $r = \sigma_1/\sigma_2$ between the inner and the outer surface, the thickness w, the ionic strength of the bathing solution, and the dielectric response of all the media involved. The latter in fact represents the biggest challenge, as the dielectric response of capsid proteins in the optical and UV regime of frequencies, which contributes most to vdW interactions, is simply not known because of the unavailable details of the electronic structure of large capsid proteins (W.-Y. Ching, personal communication; and Ref. [46]).

The variation of the charge ratio r can be seen as a proxy for the pH dependence of both surface charge densities in a more complete theory of virus shell electrostatics, which would consistently include also *charge regulation* of the capsid proteins [19,47,48]. Charge regulation refers to the details of the protonation-deprotonation equilibria at the dissociable sites of the capsid proteins amino acids as formalized in the seminal work of Ninham and Parsegian [49] and formulated within the PB theory of electrostatic interactions [7]. In this theory the charges are not assumed to be fixed, but to respond to pH and salt concentration changes.

While some partial dielectric data for bovine serum albumin do exist and were used by Roth *et al.* [50] to calculate the Hamaker coefficient of protein-protein vdW interactions, no full spectral data for capsid proteins are available [12]. We thus approximate the frequency-dependent dielectric response of capsid proteins, $\varepsilon_p(i\zeta)$, by that of hydrocarbons with four ultraviolet relaxation frequencies (for details see Ref. [8]). Without detailed capsid protein spectral data this is the best thing we can do. For numerical computations we then use the standard forms for the frequency-dependent dielectric response of water, $\varepsilon_w(i\zeta)$, described with one microwave relaxation frequency, five infrared relaxation frequencies, and six ultraviolet relaxation frequencies [51].

The additive renormalization of the surface tension and spontaneous curvature can then be cast in the form

$$\sigma \longrightarrow \sigma_0 + \frac{K_c}{R_0^2} + \frac{k_B T}{2\pi w^2}\left(\mathcal{H} + \frac{1}{(\kappa\ell_B)}\left(\frac{w}{\ell_{GC}}\right)^2\left[\frac{\frac{\varepsilon_p}{\varepsilon_w}(r+1)^2 + (\kappa w)(r^2+1)}{2\frac{\varepsilon_p}{\varepsilon_w} + (\kappa w)}\right]\right), \tag{30}$$

$$\frac{1}{R_0} \longrightarrow \frac{1}{R_0} + \frac{(k_B T/K_c)}{8\pi w}\left(\mathcal{H}' + \frac{2}{(\kappa\ell_B)}\left(\frac{w}{\ell_{GC}}\right)^2\left[\frac{\left(3\frac{\varepsilon_p}{\varepsilon_w} + 2(\kappa w) - 1\right) + 2\frac{\varepsilon_p}{\varepsilon_w}r - \left(\frac{\varepsilon_p}{\varepsilon_w} - 1\right)r^2}{2\frac{\varepsilon_p}{\varepsilon_w} + (\kappa w)}\right]\right). \tag{31}$$

Above we have introduced the Gouy-Chapman length pertaining to the outer surface charge density σ_2 as $\ell_{GC} = 1/(2\pi\ell_B(\sigma_2/e_0))$ and the Bjerrum length $\ell_B = e_0^2/(4\pi\varepsilon\varepsilon_0 k_B T)$, with $r = \sigma_1/\sigma_2$. Numerically the Bjerrum length in water equals 0.74 nm. The above form of the additive renormalization of the spontaneous curvature has a minimal value at $r_{\min} = \varepsilon_p/(\varepsilon_p - \varepsilon_w)$, whereas the renormalized surface tension is monotonic in r. These are the final expressions for the surface tension and spontaneous curvature renormalization.

Two "Hamaker coefficients" pertaining to the zeroth- and first-order curvature expansion, $\mathcal{H}$ and $\mathcal{H}'$, are obtained by assuming a symmetric configuration, where water is on both sides of the proteinaceous shell, i.e.,

$$\mathcal{H} = \sum_{N=0}^{\infty}{}' \int_0^{\infty} dx\, x \ln(1 - \Delta_{wp}(i\zeta_N)^2 e^{-2x}) = -\frac{1}{4}\sum_{N=0}^{\infty}{}' \mathrm{Li}_3(-\Delta_{wp}(i\zeta_N)^2), \tag{32}$$

$$\begin{aligned}\mathcal{H}' &= \sum_{N=0}^{\infty}{}' \tilde{f}_1(\Delta_{wp}(i\zeta_N)\Delta_{pw}(i\zeta_N), \Delta_{wp}(i\zeta_N) + \Delta_{pw}(i\zeta_N)) \\ &= \sum_{N=0}^{\infty}{}'\left[\int_0^{\infty} dx \ln(1 - \Delta_{wp}(i\zeta_N)^2 e^{-2x}) - \int_0^{\infty} dx \frac{\Delta_{wp}(i\zeta_N)^2 e^{-2x}}{1 - \Delta_{wp}(i\zeta_N)^2 e^{-2x}}(x^2 - x)\right].\end{aligned} \tag{33}$$

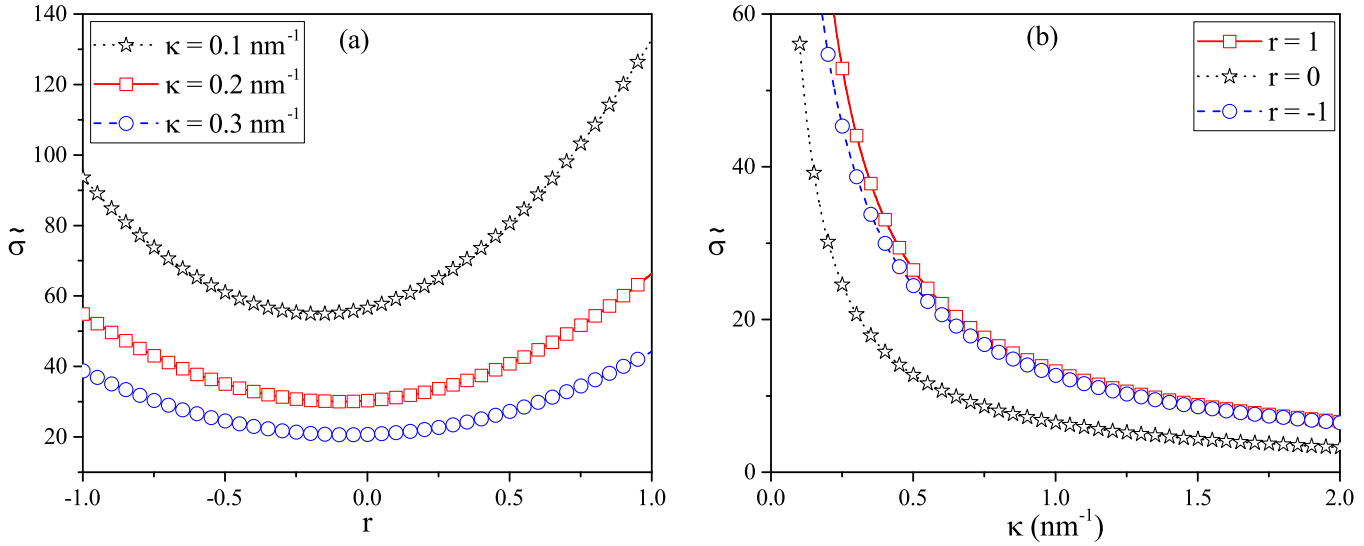

FIG. 1. Dependence of the dimensional scaling functions $\tilde{\sigma}$, Eq. (34), the surface charge ratio, $r = \sigma_1/\sigma_2$, and different values of the inverse screening length, κ. The renormalized surface tension is always positive and tends to 0 for large screening but shows nonmonotonic dependence on the charge asymmetry ratio.

With the standard water dielectric spectra [51] and hydrocarbon spectra [8] taking the place of the unknown protein dielectric spectra, this yields $\mathcal{H} \simeq -0.177$ and $\mathcal{H}' \simeq -0.386$, where the Matsubara summation included the first 500 terms.

Empty viral capsids tend to have at least a slightly negative outer shell [43]. There is more diversity concerning the charge on the inner shell, which can be negatively or positively charged. The inclusion of disordered N-tails of the capsid proteins in the charge statistics noticeably shifts the inner shell charge towards more positive values. This is especially relevant in the case of ssRNA viruses, where the disordered N-tails contribute significantly to the strongly positively charged interior, and where the charge is correlated with the genome length due to the nonspecific electrostatic interactions acting as an assembly mechanism [44,53,54].

In addition, models of multishell capsids in the presence of N-tails have highlighted the importance of charged tails in determining the capsid size, which can, in multishell conformations, differ from the capsid's preferred (spontaneous) radius of curvature, due to the interplay of eletrostatic repulsion between the tails and attraction between the tails and the outer surface of the neighboring shell [55]. While we simply assign the contribution of the N-tails to the inner surface charge density σ_2 in order to keep our model consistent, we thus consider the possibility that σ_2 has either negative or positive sign, the latter stemming from the contribution of the positively charged tails to the inner charge.

The inner and outer surface charge density of the virus capsids is in general quite high compared with those of other charged biomolecules, being in the range $[-0.4,0.4]$ e_0/nm^2. Invoking the previously obtained average capsid radii this implies net charge values in the range $\sim 4500 e_0$ [52]. The exact values of the surface charge density depend on the charge model, i.e., single- vs double-shell models, and on the presence of the charged N-tails as discussed above (for details see Ref. [43]). We thus introduce the charge asymmetry parameter as the ratio of inner and outer surface charges, $r = \sigma_1/\sigma_2$, and, in the following, consider the range $r \in [-1,1]$.

According to the above statistics of virus charges the Gouy-Chapman length corresponding to 0.4 e_0/nm^2 is $\ell_{\mathrm{GC}} = 0.54$ nm, while the outer-inner charge ratio spans $-1 < r < 1$. For more than 75% of viruses analyzed in Ref. [43], the thickness is confined to a narrow range, $w \simeq 1.5$–4.5 nm, with $w \simeq 3$ nm a good estimate of the average. The monovalent salt concentration can be taken in the typical range 0.001–1 M, which amounts to Debye lengths of 10.75–0.34 nm.

In order to understand the consequences of spontaneous curvature renormalization we rewrite Eqs. (30) and (31) in a form that contains only the interaction renormalized part

$$\sigma = \frac{k_B T}{w^2}\tilde{\sigma} \quad \text{with}$$
$$\tilde{\sigma} = \frac{\mathcal{F}_0((\kappa\ell_B),(w/\ell_{\mathrm{GC}}),\kappa w,r)}{2\pi(\kappa\ell_B)(\kappa\ell_{\mathrm{GC}})^2}, \tag{34}$$
$$\frac{1}{R_0} = \frac{(k_B T/K_c)}{w}\frac{1}{\tilde{R}_0} \quad \text{with}$$
$$\frac{1}{\tilde{R}_0} = \frac{\mathcal{F}_1((\kappa\ell_B),(w/\ell_{\mathrm{GC}}),\kappa w,r)}{8\pi(\kappa\ell_B)(\kappa\ell_{\mathrm{GC}})^2}, \tag{35}$$

where $\tilde{\sigma}$ and $\tilde{R}_0$ are now dimensionless contributions to the surface tension and spontaneous curvature due to DLVO interactions. The surface tension and spontaneous curvature obviously have the scale of $k_B T/w^2$ and $(k_B T/K_c)/w$, respectively. For the former it amounts to a fraction of the surface tension of water ($\sim$0.5–4 pN/nm), and for the latter it is within the range of the capsid radii (10–100 nm), obtained from the estimated values of the capsid elasticity [52]. $\mathcal{F}_{0,1}((\kappa\ell_B),(w/\ell_{GC}),\kappa w,r)$ are complicated dimensionless scaling functions. Alternatively, they can be written in the form $\mathcal{F}_{0,1}((\kappa\ell_B)(\kappa\ell_{GC})^2,\kappa w,r)$. The salient features of dimensionless contributions to the surface tension

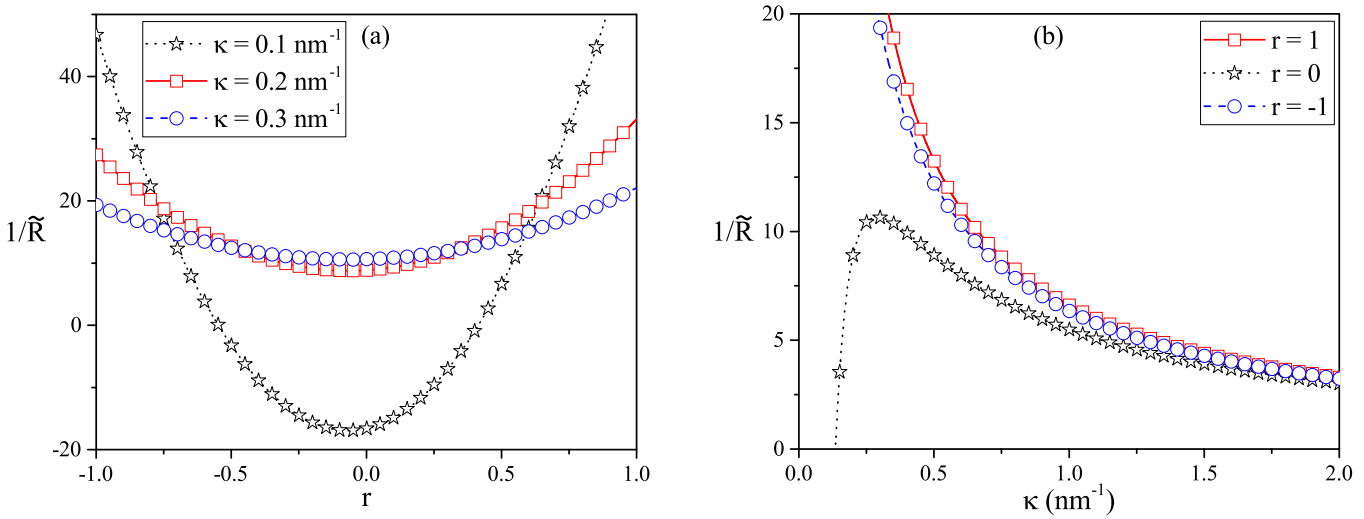

FIG. 2. Dependence of the dimensional scaling function, $1/\tilde{R}_0$, Eq. (35), on the surface charge ratio, $r = \sigma_1/\sigma_2$, and different values of the inverse screening length, κ. The renormalized curvature is in general a nonmonotonic function of r and κ and can be of either sign, depending on the charge asymmetry parameter and the amount of screening in the system.

and spontaneous curvature are presented in Fig. 1 and Fig. 2.

Figure 1 shows that the DLVO interaction renormalized surface tension tends, in a monotonic way, to the bare value as the screening length is decreased, i.e., salt is added to the system, and is always positive, irrespective of the detailed values of the interaction parameters. The dependence on the charge ratio is more complicated and in general leads to nonmonotonic behavior. The charge asymmetry thus engenders a minimum in the interaction renormalized surface tension, whose depth depends on the amount of screening present in the system.

Figure 2 shows analogous dependencies for the DLVO interaction renormalized curvature, but in this neither of the dependencies is monotonic. While the dependence on the charge asymmetry again shows a pronounced minimum at $r_{\min} = \varepsilon_p/(\varepsilon_p - \varepsilon_w)$, whose depth depends on the salt screening, the dependence on the inverse Debye length can be either monotonic, when $r \sim \pm 1$, or nonmonotonic, when it is close to $r_{\min}$. Furthermore, depending on the charge asymmetry parameter, the interaction renormalized spontaneous curvature can be either positive or negative. In the above numerical analysis we have not considered explicitly the variation of the dielectric spectrum of the capsid proteins, as very little is presently known of its details.

IV. CONCLUSION

Motivated by recent experiments revealing that electrostatic interactions can be of paramount importance for the morphology of capsid-like aggregates and can fundamentally change the phase diagram of, e.g., the CCMV capsid protein, where, besides regions of single-wall and multiwall capsids, tubes and free protein regions can be observed as a function of the electrolyte solution parameters [3], we derived an interaction renormalization of the elastic properties of a proteinaceous shell of the virus capsid type. The interaction potentials taken into account are of the DLVO type and, by assumption, composed of the vdW and electrostatic part. The first one considered at the level of the Lifshitz theory, and the second one at the level of the linearized PB theory. This formulation of the problem then hinges only on mesoscale parameters characterizing the shell, such as the dielectric function of the capsid proteins, magnitude of the dielectric discontinuity at the capsid-aqueous solvent boundary, capsid thickness, Debye screening length, and inner and the outer surface charge densities. Just as in the case of the DLVO theory of the stability of colloids, microscopic details are not necessary to calculate the effect of the solution parameters on the magnitude of the spontaneous curvature.

The approach advocated here, avoiding all the microscopic details of the capsid shell composition, such as the internal structure of its proteins, possible nonisotropic dielectric response, and detailed distribution of charged sites, obviously bypasses more detailed microscopic calculations, starting from the interaction free energy between capsomeres and its dependence on their mutual orientation, which could eventually be translated into the spontaneous curvature of the shell. Just as more microscopic approaches to the colloid stability problem illuminate the mesoscale parameters used in the macroscopic DLVO approach, they could also fill in the details of our macroscopic description of proteinaceous shells and our theory could, in principle, be refined, but with much effort and with the introduction of new, completely unknown and unquantified properties, like the anisotropic dielectric function of the proteinaceous shell, the inclusion of detailed charge dissociation equilibria for all the (de)protonated amino acids [19], or even the explicit introduction of the non-DLVO interactions such as hydration and hydrophobic interactions [9]. We are convinced at this point that such a generalization, even if possible, would not clarify the problem but make it completely untransparent and unquantifiable. The thickness of the proteinaceous shell, confined to the narrow range of $\simeq$1.5–4.5 nm [43] and comparable to the thickness of

the lipid bilayers, does make our approach susceptible to criticism regarding the limitations of the continuum approach. While this criticism could be relevant, one should not gloss over different types of drawbacks of at-first-glance "exact" results, which could be provided by more detailed molecular simulations, based, however, on molecular potentials, which, as a rule, compare poorly with the measured interaction potentials between (bio)macromolecules. Before model molecular potentials reach maturity, interim continuum results, which can be expected to be qualitatively relevant, if not quantitatively predictive, are the best we can do.

While the calculation of the surface tension and spontaneous curvature renormalization by the long-range DLVO potentials at the mesoscale level leaves no ambiguities in the results, the calculation of the renormalized bending rigidity is more sensitive to the detailed assumptions regarding the neutral surface with respect to which one renormalizes the long-range interaction part of the free energy. This is why we took the bending rigidity as a phenomenological parameter determined by the experiment.

ACKNOWLEDGMENTS

H.R.S. and M.M. acknowledge support from NSF Grant No. DMR-1404940. R.P. acknowledge support in the study of long-range interactions for biomolecular and inorganic nanoscale assembly by the U.S. Department of Energy, Office of Basic Energy Sciences, Division of Materials Sciences and Engineering under Award No. DE-SC0008176.

APPENDIX

We define the *Lerch transcendental* function in the standard form as

$$\Phi(z,s,v) = \sum_{n=0}^{\infty} \frac{z^n}{(v+n)^s}. \tag{A1}$$

Obviously the polylog function can be expressed as $\mathrm{Li}_s(z) = z\Phi(z,s,1)$, and the more familiar Riemann zeta function then follows as $\zeta(s) = \mathrm{Li}_s(1) = \Phi(1,s,1)$. The analytical continuation of the Lerch function is particularly appropriate for evaluation of the integrals that figure in the vdW part of the spheroidal shell free energy expansion.

In fact the exact expressions that we use in the section on the vdW free energy curvature expansion are of the form

$$\int_0^{\infty} dx\, x \log\left(1+\Delta^* e^{-2x}\right) = -\frac{1}{4}\mathrm{Li}_3(\Delta^*) \tag{A2}$$

as well as

$$\int_0^{\infty} \frac{dx\, x^{v-1} e^{-2x}}{1+\Delta^* e^{-2x}} = \frac{1}{2^v}\Gamma(v)\Phi(-\Delta^*,v,1) \tag{A3}$$

and

$$\int_0^{\infty} \frac{dx\, x^{v-1} e^{-4x}}{(1+\Delta^* e^{-2x})^2} = \frac{1}{2^v}\Gamma(v)[\Phi(-\Delta^*,v-1,2) - \Phi(-\Delta^*,v,2)]. \tag{A4}$$

We use the Lerch transcendental function to obtain values of all the integrals in the curvature expansion of the vdW interaction energy.

[1] L. Lavelle, M. Gingery, W. M. Gelbart, and C. M. Knobler, J. Phys. Chem. B **113**, 3813 (2009).
[2] A. Šiber, A. Losdorfer Bozic, and R. Podgornik, Phys. Chem. Chem. Phys. **14**, 3746 (2012).
[3] J. R. Vega-Acosta, R. D. Cadena-Nava, W. M. Gelbart, C. M. Knobler, and J. Ruiz-García, J. Phys. Chem. B **118**, 1984 (2014).
[4] A. Šiber and A. Majdandzić, Phys. Rev E **80**, 021910 (2009).
[5] J. Wagner and R. Zandi, Biophys. J. **109**, 956 (2015).
[6] K. J. M. Bishop, C. E. Wilmer, S. Soh, and B. A. Grzybowski, Small **5**, 1600 (2009).
[7] T. Markovich, D. Andelman, and R. Podgornik, in *Handbook of Lipid Membranes*, edited by C. Safynia and J. Raedler (Taylor & Francis, New York, 2016).
[8] V. A. Parsegian, *vdW Forces* (Cambridge University Press, Cambridge, UK, 2005).
[9] R. H. French, V. A. Parsegian, R. Podgornik *et al.*, Rev. Mod. Phys. **82**, 1887 (2010).
[10] J. N. Israelachvili, *Intermolecular and Surface Forces*, 3rd ed. (Academic Press, London, 2011).
[11] N. I. Lebovka, in *Advances in Polymer Science, Vol. 255*, edited by M. Müller (Springer, Berlin, 2014), p. 57.
[12] L. M. Woods, D. A. R. Dalvit, A. Tkatchenko, P. Rodriguez-Lopez, A. W. Rodriguez, and R. Podgornik, Rev. Mod. Phys. (2016), arXiv:1509.03338 [cond-mat.mtrl-sci].
[13] E. E. Meyer, K. J. Rosenberg, and J. Israelachvili, Proc. Natl. Acad. Sci. USA **103**, 15739 (2006).
[14] P. Ceres and A. Zlotnick, Biochemistry **41**, 11525 (2002).
[15] W. K. Kegel and P. van der Schoot, Biophys J. **86**, 3905 (2004).
[16] V. A. Parsegian and B. W. Ninham, Biophys. J. **10**, 664 (1970).
[17] A. Naji, M. Kanduč, J. Forsman, and R. Podgornik, J. Chem. Phys. **139**, 150901 (2013).
[18] M. Lund and B. Jönsson, Q. Rev. Biophys. **46**, 265 (2013).
[19] R. J. Nap, A. Losdorfer Bozic, I. Szleifer, and R. Podgornik, Biophys. J. **107**, 1970 (2014).
[20] D. M. Leneveu, R. P. Rand, V. A. Parsegian, and D. Gingell, Biophys. J. **18**, 209 (1977).
[21] T. T. Nguyen, R. F. Bruinsma, and W. M. Gelbart, Phys. Rev. E **72**, 051923 (2005).
[22] M. Deserno, Chem. Phys. Lipids **185**, 11 (2015).
[23] Y. Andoh, K. Oono, S. Okazaki, and I. Hatta, J. Chem. Phys. **136**, 155104 (2012).
[24] M. Winterhalter and W. Helfrich, J. Phys. Chem. **92**, 6865 (1988); **96**, 327 (1992).
[25] D. J. Mitchell and B. W. Ninham, Langmuir **5**, 1121 (1989).
[26] H. N. W. Lekkerkerker, Physica A **167**, 384 (1990).
[27] B. Duplantier, R. E. Goldstein, V. Romero-Rochin, and A. I. Pesci, Phys. Rev. Lett. **65**, 508 (1990).
[28] B. Duplantier, Physica A **168**, 179 (1990).

[29] T. Chou, M. V. Jarić, and E. D. Siggia, Biophys. J. **72**, 2042 (1997).
[30] V. Kumaran, Phys. Rev. E **64**, 051922 (2001).
[31] L. Javidpour, A. Lošdorfer Božič, A. Naji, and R. Podgornik, J. Chem. Phys. **139**, 154709 (2013).
[32] V. A. Parsegian and G. H. Weiss, J. Chem. Phys. **60**, 5080 (1974).
[33] D. S. Dean and R. R. Horgan, Phys. Rev. E **73**, 011906 (2006).
[34] H. Kleinert, Phys. Lett. A **136**, 253 (1989).
[35] N. S. Witte, J. Chem. Phys. **99**, 8168 (1993).
[36] A. W. C. Lau and P. Pincus, Phys. Rev. Lett. **81**, 1338 (1998).
[37] R. R. Netz, Phys. Rev. E **64**, 051401 (2001).
[38] D. S. Dean and R. R. Horgan, Phys. Rev. E **71**, 041907 (2005).
[39] S. A. Safran, *Statistical Thermodynamics of Surfaces, Interfaces, and Membranes* (Addison-Wesley, Reading, MA, 1994).
[40] R. Podgornik, P. L. Hansen, and V. A. Parsegian, J. Chem. Phys. **113**, 9343 (2000).
[41] J. C. Hopkins, D. M. Dryden, W.-Y. Ching, R. H. French, V. A. Parsegian, and R. Podgornik, J. Colloid Interf. Sci. **417**, 278 (2014).
[42] A. Šiber and R. Podgornik, Phys. Rev. E **76**, 061906 (2007).
[43] A. Losdorfer Bozic, A. Siber, and R. Podgornik, J. Biol. Phys. **38**, 657 (2012).
[44] V. A. Belyi and M. Muthukumar, Proc. Natl. Acad. Sci. USA **103**, 17174 (2006).
[45] D. Andelman, in *Handbook of Physics of Biological Systems, Vol. 1*, edited by R. Lipowsky and E. Sackman (Elsevier Science, Amsterdam, 1995), Chap. 12.
[46] F. Pichierri, arXiv:1107.5853v1 [q-bio.BM].
[47] H. K. Lin, P. P. A. M. van der Schoot, and R. Zandi, Phys. Biol. **9**, 066004 (2012).
[48] R. Kusters, L. Hsiang-Ku, R. Zandi, I. Tsvetkova, B. Dragnea, and P. van der Schoot, J. Phys. Chem. B **119**, 1869 (2015).
[49] B. W. Ninham and V. A. Parsegian, J. Theor. Biol. **31**, 405 (1971).
[50] C. M. Roth, B. L. Neal, and A. M. Lenhoff, Biophys. J. **70**, 977 (1996).
[51] R. R. Dagastine, D. C. Prieve, and L. R. White, J. Colloid Interf. Sci. **231**, 351 (2000).
[52] A. Lošdorfer Božič, A. Šiber, and R. Podgornik, J. Biol. Phys. **39**, 215 (2013).
[53] C. L. Ting, J. Wu, and Z. G. Wang, Proc. Natl. Acad. Sci. USA **108**, 16986 (2011).
[54] P. Ni, Z. Wang, X. Ma, N. C. Das, P. Sokol, W. Chiu, B. Dragnea, M. Hagan, and C. Cheng Kao, J. Mol. Biol. **419**, 284 (2012).
[55] P. Prinsen, P. van der Schoot, W. M. Gelbart, and C. M. Knobler, J. Phys. Chem. B **114**, 5522 (2010).